Analysis of uncertainties in future climate projections for South America: comparison of WCRP-CMIP3 and WCRP-CMIP5 models

Josefina Blázquez & Mario N. Nuñez

Climate Dynamics
Observational, Theoretical and Computational Research on the Climate System

ISSN 0930-7575
Volume 41
Combined 3-4

Clim Dyn (2013) 41:1039-1056
DOI 10.1007/s00382-012-1489-7

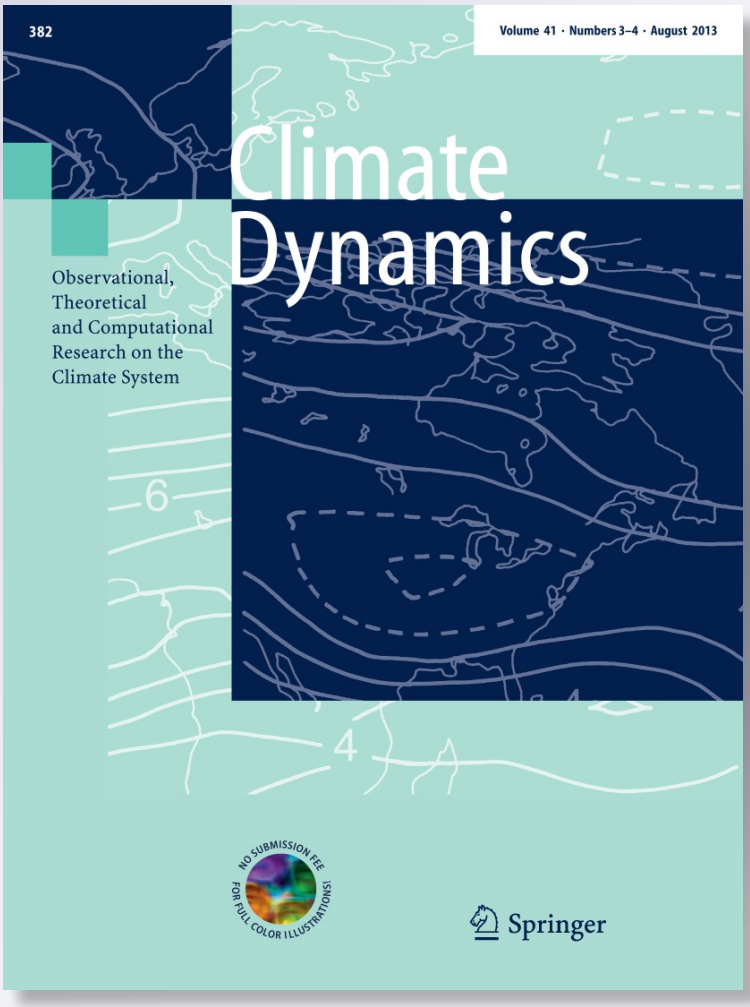

Springer

Clim Dyn (2013) 41:1039–1056
DOI 10.1007/s00382-012-1489-7

Analysis of uncertainties in future climate projections for South America: comparison of WCRP-CMIP3 and WCRP-CMIP5 models

Josefina Blázquez · Mario N. Nuñez

Received: 9 May 2012 / Accepted: 10 August 2012 / Published online: 29 August 2012

Abstract This paper identifies two sources of uncertainties in model projections of temperature and precipitation: internal and inter-model variability. Eight models of WCRP-CMIP3 and WCRP-CMIP5 were compared to identify improvements in the reliability of projections from new generation models. While no significant differences are observed between both datasets, some improvements were found in the new generation models. For example, in summer CMIP5 inter-model variability of temperature was lower over northeastern Argentina, Paraguay and northern Brazil, in the last decades of the 21st century. Reliability of temperature projections from both sets of models is high, with signal to noise ratio greater than 1 over most of the study region. Although no major differences were observed in both precipitation datasets, CMIP5 inter-model variability was lower over northern and eastern Brazil in summer (especially at the end of the 21st century). Reliability of precipitation projections was low in both datasets. However, the signal to noise ratio in new generation models was close to 1, and even greater than 1 over eastern Argentina, Uruguay and southern Brazil in some seasons.

Keywords Uncertainties · Projections · South America · CMIP3 models · CMIP5 models

Abbreviations

WCRP	World Climate Research Program
CMIP	Coupled Model Intercomparison Project
SRES	Special Report on Emission Scenarios
RCP	Representative Concentrations Pathways
SESA	Southeastern South America
ITCZ	Intertropical Convergence Zone
SACZ	South Atlantic Convergence Zone

1 Introduction

Uncertainty is a common feature in global climate model projections for various regions of the world and particularly evident in some parts of South America. It is very important that decision makers are informed about the reliability of future climate projections, so they can adequately design adaptation policies. This paper analyses uncertainties in future climate projections for South America for some decades of the 21st century in detail.

Sources of uncertainty need to be identified and differentiated, given that uncertainties vary with the variables, the projection times and emission scenarios. There are three main sources of uncertainty: internal variability (the result of natural variations occurring in absence of external forcing), inter-model variability (under the same forcing, each model simulates different climate changes) and the variability between emission scenarios (each scenario

J. Blázquez (✉) · M. N. Nuñez
Centro de Investigaciones del Mar y la Atmósfera (CIMA-CONICET/FCENUBA), Ciudad Universitaria Pabellón II Piso 2, C1428EGA, Buenos Aires, Argentina
e-mail: blazquez@cima.fcen.uba.ar

M. N. Nuñez
e-mail: mnunez@cima.fcen.uba.ar

J. Blázquez · M. N. Nuñez
Departamento de Ciencias de la Atmósfera y los Océanos (FCEN-UBA), Ciudad Universitaria Pabellón II Piso 2, C1428EGA, Buenos Aires, Argentina

J. Blázquez · M. N. Nuñez
Instituto Franco Argentino del Clima y sus Impactos (UMI IFAECI/CNRS), Ciudad Universitaria Pabellón II Piso 2, C1428EGA, Buenos Aires, Argentina

represents a different amount of future greenhouse gas emissions).

Recently, Hawkins and Sutton (2009) (hereafter HS09) and Hawkins and Sutton (2011) (hereafter HS11) showed that, globally, internal variability is the greatest source of uncertainty in near future temperature and precipitation projections. On the other hand, projections for the end of the century are dominated by inter-model variability. This can be clearly seen in precipitation projections. In addition, Giorgi and Francisco (2000) found that the greatest uncertainty in regional climate projections is associated with the spread among models. Other studies quantified different types of uncertainty for different regions using different methods (Giorgi and Bi 2009; Knutti et al. 2008; Cox and Stephenson 2007; Murphy et al. 2004; Giorgi and Mearns 2002; among others).

There are numerous studies on climate change projections for South America from global models (Labraga and Lopez 1997; Carril et al. 1997; Bidegain and Camilloni 2006; Vera et al. 2006; Kitoh et al. 2011; Blázquez et al. 2012, among others) and regional models (Garreaud and Falvey 2008; Soares and Marengo 2008; Nuñez et al. 2009; Marengo et al. 2009a, b; Urrutia and Vuille 2009; Cabré et al. 2010; Marengo et al. 2011, among others). However, uncertainties associated with those projections have not been studied in depth. Vera et al. (2009) is one of the few studies addressing this issue. They found that temperature (precipitation) changes projected by the WCRP-CMIP3 models are significantly greater (less) than inter-model variability. This paper attempts to quantify the uncertainties associated with future climate projections (caused by both internal and inter-model variability) over South America, to identify where temperature and precipitation projections are more reliable. These results will provide decision makers with more reliable information for climate change adaptation measures and will identify the greatest sources of uncertainty in projections to try to reduce them.

2 Data

Uncertainties were examined in future climate projections from models of the World Climate Research Programme's (WCRPs) Coupled Model Intercomparison Project phase 3 (CMIP3) and phase 5 (CMIP5) (Tables 1, 2). The main differences between these packages of models are summarized in "Appendix". The simulations used in the case of CMIP3 models are 20c3m for present and SRES A1B (Special Report on Emission Scenarios, Nakicenovic et al. 2000) for the future. More details on these simulations are available in Meehl et al. (2007). In the case of CMIP5 models, historical experiments were used for the present and RCP45 (Representative Concentrations Pathways, Moss et al. 2008, 2010) for the future (further details in Taylor et al. 2012). The 8 models from CMIP5 dataset that were available at the moment of starting this analysis (CMIP5 experiments were made available in July 2011) are presented here.

The new generation models were obtained using new emissions scenarios called RCPs. These scenarios were constructed since the previous (SRES) were created about 10 years ago. The new scenarios have information about new socioeconomic data, emerging technologies and observations of environmental factors such as land use and land cover change (Moss et al. 2010). In particular the new scenario chosen in this paper is the RCP45, which is a stabilization scenario, i.e. achieves a level of radiative forcing of 4.5 W/m^2 in 2100 (which is equivalent to a CO_2 concentration of 550 ppm). It is worth mentioning that the concentrations of this new scenario are slightly lower than in the SRESA1B (720 ppm by the year 2100). Last but not least, it is worth clarifying that for this study it would be better to compare the same scenarios to attribute differences only to models. But as it was said previously CMIP5 models were run using the new generation of emission scenarios (RCP). Anyway, this comparison is worthwhile because it is widely known that the precipitation is the variable with larger uncertainty in future projections and it has been proved in HS09 and HS11 that precipitation is not (or it is less) sensitive to the emission scenario than temperature.

3 Methodology

Simulations were interpolated to a common grid of $2.5° \times 2.5°$ prior to analysis to make projections from models with different horizontal resolutions comparable (Tables 1 and 2). Only one simulation from each of CMIP3 and CMIP5 model and one emission scenario (A1B for CMIP3 and RCP45 for CMIP5) were used in this study. Sources of uncertainty were divided into internal variability and inter-model variability following the methodology described in HS09. The present analysis has not considered the variability between emission scenarios, because of the lack of data from CMIP5 experiments and because the most relevant sources of uncertainty in precipitation projections (the variable with the greatest uncertainty) are internal and inter-model variability (HS11). The methodology used to break up the sources of uncertainty into individual components is described in "Appendix" of HS09, and summarized below.

Uncertainty caused by internal and inter-model variability was calculated by adjusting raw data to a fourth order polynomial,

Table 1 WCRP-CMIP3 models used in the study

Model name	Institution (country)	Resolution (°lat × °lon)	Reference
CGCM3.1(T63)	Canadian Center for Climate Modeling and Analysis (Canada)	Atm: T63 (~1.9° × 1.9°) Oce: 0.9° × 1.4°	Flato (2005)
CSIRO-MK3.0	CSIRO Atmospheric Research (Australia)	Atm: T63 (~1.9° × 1.9°) Oce: 0.8° × 1.9°	Gordon et al. (2002)
INM-CM3.0	Institute for Numerical Mathematics (Russia)	Atm: 5° × 4° Oce: 2° × 2.5°	Volodin and Diansky (2004)
IPSL-CM4	Institut Pierre Simon Laplace (France)	Atm : 2.5° × 3.75° Oce : 2° × 2°	Marti et al. (2005)
MIROC3.2 (hires)	Cent. for Clim. Sys. Res, Univ of Tokyo, Nat. Inst. for Envir. Studies & Frontier Res. Cent. For Global Change (Japan)	Atm: T101(~1.1° × 1.1°) Oce: 0.2° × 0.3°	Hasumi et al. (2004)
MIROC3.2 (medres)	Cent. for Clim. Sys. Res, Univ of Tokyo, Nat. Inst. for Envir. Studies & Frontier Res. Cent. For Global Change (Japan)	Atm: T42 (~2.8° × 2.8°) Oce: 0.5°–1.4° × 1.4°	Hasumi et al. (2004)
MRI-CGCM2.3.2	Meteorological Research Institute (Japan)	Atm: T42 (~2.8° × 2.8°) Oce: 0.5–2° × 2.5°	Yukimoto and Noda (2002)
UKMO HadGEM1	Hadley Centre for Climate Prediction and Research/ Met Office (United Kingdom)	Atm: ~1.3° × 1.9° Oce: 0.3°–1° × 1°	Johns et al. (2006)

Table 2 WCRP-CMIP5 models used in the study

Model name	Institution (country)	Resolution (°lat × °lon)	Reference
CanESM2	Canadian Centre for Climate Modelling and Analysis (Canada)	Atm: T63 (~1.9° × 1.9°) Oce: 0.9° × 1.4°	Chylek et al. (2011)
CSIRO-Mk3.6	Commonwealth Scientific and Industrial Research Organisation and the Queensland Climate Change Centre of Excellence (Australia)	Atm: T63 (~1.9° × 1.9°) Oce: 0.9° × 1.9°	Rotstayn et al. (2010)
INM-CM4	Institute for Numerical Mathematics (Russia)	Atm: 1.5° × 2° Oce: 0.5° × 1°	Volodin et al. (2010)
IPSL-CM5A-LR	Institut Pierre-Simon Laplace (France)	Atm: 1.9° × 3.75° Oce: 1.2° × 2°	http://icmc.ipsl.fr/images/internal/ipsl-esm-20100228-1.pdf
MIROC5	Atmosphere and Ocean Research Institute (The University of Tokyo), National Institute for Environmental Studies, and Japan Agency for Marine-Earth Science and Technology (Japan)	Atm: T85 (~1.4° × 1.4°) Oce: 1° × 1°	Watanabe et al. (2010)
MIROC-ESM	Atmosphere and Ocean Research Institute (The University of Tokyo), National Institute for Environmental Studies, and Japan Agency for Marine-Earth Science and Technology (Japan)	Atm: T42 (~2.8° × 2.8°) Oce: 1° × 1.4°	Watanabe et al. (2011)
MRI-CGCM3	Meteorological Research Institute (Japan)	Atm: T159 (~1.125° × 1.125°) Oce: 0.5° × 1°	Yukimoto et al. (2011)
HadGEM2-ES	Met Office Hadley Centre (United Kingdom)	Atm: N96 (~1.25° × 1.875°) Oce: 1°–0.3° × 1°	Martin et al. (2011) Collins et al. (2009)

$$X_{m,t} = x_{m,t} + r_{m,t} \quad (1)$$

where $X_{m,t}$, raw data; $x_{m,t}$ data adjusted by the fourth order polynomial; $r_{m,t}$ the residual (difference between raw and adjusted data). Subscripts m and t denote models and seasons, respectively.

The two sources of variability were defined using the new variables. An example of raw and adjusted data for

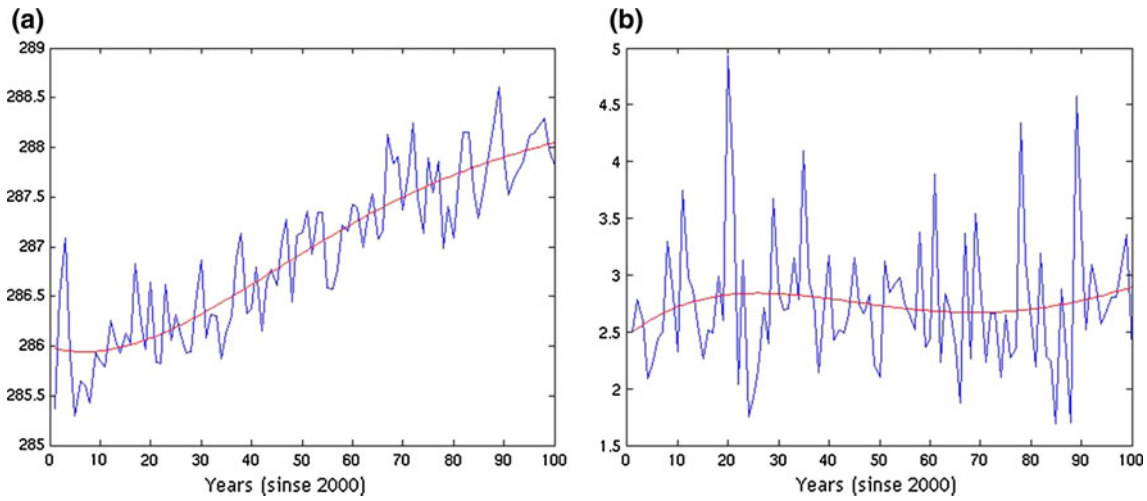

Fig. 1 Row data (*blue line*) and adjusted data (*red line*). **a** Temperature (K), **b** precipitation (mm/day). Example for a CMIP3 model, for one grid point, for the summer

both temperature and precipitation is shown in Fig. 1. Internal variability (V_i) was defined as follows:

1. The average of residuals of each model and decade in the periods 2001–2100 for CMIP3 models and 2011–2100 for CMIP5 models.
2. The variance between decades was calculated for each model
3. Variances obtained for each model were averaged.

The result of this procedure is a V_i that remains constant throughout the 21st century. Although the distribution of internal variability may vary in the future (Solomon et al. 2007), it is assumed to remain constant throughout the current century (i.e., it is not affected by the increase in greenhouse gases). For more information of this assumption, see HS09.

Inter-model variability (V_m) was calculated from the adjusted data as follows:

$$Vm(t) = \frac{\sum_m (A_m(t) - M_m(t))^2}{N} \quad (2)$$

where $A(t)$ is the anomaly of temperature or precipitation (adjusted data) relative to the average 1971–2000, for each model and each decade of the century. Anomalies were calculated for each model in order to avoid uncertainties caused by the climatologies generated by the different models. $M(t)$ is the average of model anomalies for each decade, and N is the number of models used. Unlike V_i, V_m varies with time.

All models were assigned the same weight, given that no major differences are observed after assigning different weights to models in previous works (HS09; Vera et al. 2009).

Both sources of uncertainty are assumed to be independent, so the total variability can be defined as:

$$V_T(t) = V_i + V_m(t) \quad (3)$$

The weight of internal variability relative to the total variability throughout the century is defined as:

$$RW(t) = \frac{V_i}{V_i + V_m(t)} \times 100 \quad (4)$$

The reliability of projections was calculated as a signal to noise ratio:

$$SN(t) = \frac{\Delta x(t)}{\sigma_T(t)} \quad (5)$$

where $\Delta x(t)$ is the signal defined as the difference between decade (t) of 21st century and the average 1971–2000. $\sigma_T(t)$ is the total standard deviation for decade (t) calculated from V_T. The reliability of changes was assessed with a Student test, after testing variances using a Fisher test (both at 95 % confidence level for temperature and precipitation).

Finally, the CMIP3 and CMIP5 multi-model datasets were compared as follows:

$$Ratio = \frac{Var(CMIP3)}{Var(CMIP5)} \quad (6)$$

where Var is the internal or inter-model variability.

4 Results

This section compares the uncertainties in future temperature and precipitation projections from 8 CMIP3 and CMIP5 models (Tables 1, 2).

It is widely known, especially in short-range forecast, that the larger the ensemble spread, the better the ensemble, i.e. when the spread of the ensemble is large is better because it has more possibility to contain the "truth". That is why in numerical weather prediction exist numerous techniques to try to find the most unstable perturbation to initialize the model. This is done to assure that the ensemble contains the "truth". On the other hand, the larger the ensemble spread, the bigger the uncertainty. So it is like a cost-benefit issue, so in this study the risk was taken and it is accepted the ensemble with less uncertainty as a better.

In this paper, seasons were defined as follow: austral summer: December–January–February, austral autumn: March–April–May, austral winter: June–July–August and austral spring: September–October–November.

4.1 Temperature

Projected decadal temperature changes (relative to the period 1971–2000) are shown in Fig. 2 (for summer and winter) and Fig. 3 (for autumn and spring), for the 3rd (2021–2030), 5th (2041–2050), 7th (2061–2070) and 9th (2081–2090) decades of the 21st century). Statistically significant positive changes are observed in all seasons (95 % confidence level) throughout the domain considered, with the highest values of change located over the continent (especially over northern Argentina and central Brazil). There is a peculiarity between both datasets that repeats in all seasons and is particularly visible in the last decades of the century: changes are greater in the CMIP3 than in the CMIP5 dataset, which could be expected, given that greenhouse gas concentrations are higher in the emission scenario used in CMIP3 models (SRESA1B). The biggest differences appear in the last decades of the current century probably because the maximum difference between both emission scenarios occurs at the end of the century. For example, the CO_2 concentration are almost the same until mid-century in both emission scenarios, after that, they begin to diverge reaching by the year 2100 720 ppm in the case of SRESA1B and 550 ppm in RCP45.

Internal variability (which was assumed to be constant over the 21st century) is shown in Fig. 4 where in all the seasons, and in both model packages two variability peaks appear: one over the northeast of Brazil and the other over northeastern Argentina and Paraguay. However, CMIP5 models locate the tropical latitude maximum further to the east. Internal variability peaks range from 0.1 to 0.14 °C and values are similar over South America, although some differences appear in some seasons. For example, in winter, the maximum located over northeastern Argentina and Paraguay is more intense in CMIP3 than in CMIP5 models; in spring CMIP3 models locate the main maximum in the northwest of Brazil, while CMIP5 models place it over northeastern Argentina and Paraguay.

Inter-model variability was also examined in both sets of models (Fig. 5 shows inter-model variability only for summer and winter, and for the 3rd, 5th, 7th and 9th decades of 21st century). In all seasons inter-model variability grows with time. The highest values are observed over tropical and sub-tropical latitudes (above 1.8 °C at the end of the century). In particular, some differences between both model packages appear in summer. There are two main peaks: one over northeastern Argentina and Paraguay and the other over the north of Brazil (regions coincide approximately with the maximum of internal variability), although these peaks are smaller in the last decades of the century in CMIP5 models. In autumn (not shown), new generation models generally perform worse than CMIP3 models, with greater inter-model variability in all the decades of the current century (except in the 9th decade, where the variability peak in CMIP3 models covers a greater area). During winter months, the location (northwest and central Brazil) and values of variability maxima are similar in both model packages. In the three first decades the area covered by the variability maximum is greater in CMIP5 models. In this season there is also another main maximum in the south of the domain (on the Atlantic and Pacific Oceans). In spring (not shown), inter-model variability in CMIP5 models is greater over northeastern Brazil in the middle of the 21st century, whereas at the end of the century variability peaks in the mentioned region are similar in both model packages. It is worth noting that the peaks of inter-model variability coincide approximately with the location of the greatest projected changes (Figs. 2, 3) in all seasons.

Figures 6 shows the relative weights (RWs) of internal variability (Eq. 4) for summer, and winter, and for the decades analysed. In all seasons, the weight of internal variability decreases with time, which would indicate that internal variability is important in the early decades and inter-model variability in the last decades of the century.

The reliability of temperature projections from CMIP3 and CMIP5 models was also compared. Figure 7 shows the signal to noise ratio (SN) for summer and winter months and for all the decades analysed. As expected, SN values were greater than 1 over most of the study domain, which indicates that temperature projections are highly reliable throughout the century. Figure also shows that SN values are higher in CMIP3 models in some regions and decades of the 21st century, which might be explained by the fact that CMIP3 models project greater temperature changes (Fig. 2).

The level of uncertainty in both datasets was compared using Eq. 6. Values above (below) 1 indicate that inter-model or internal variability in CMIP3 is larger (smaller) than in CMIP5 models. Pink (blue) indicates areas where

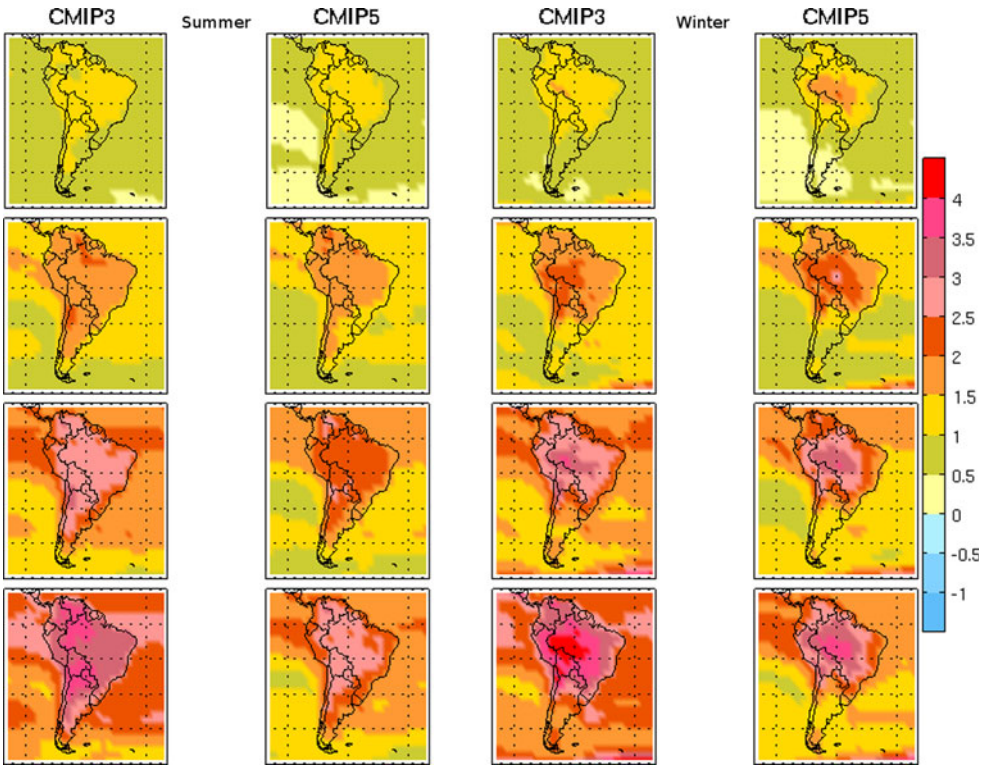

Fig. 2 Decadal mean temperature changes (relative to the average 1971–2000) (°C) for summer and winter for the CMIP3 and CMIP5 models. 95 % confidence level (*shaded*). The *rows* (from *top* to *bottom*) indicate decades 3, 5, 7 and 9

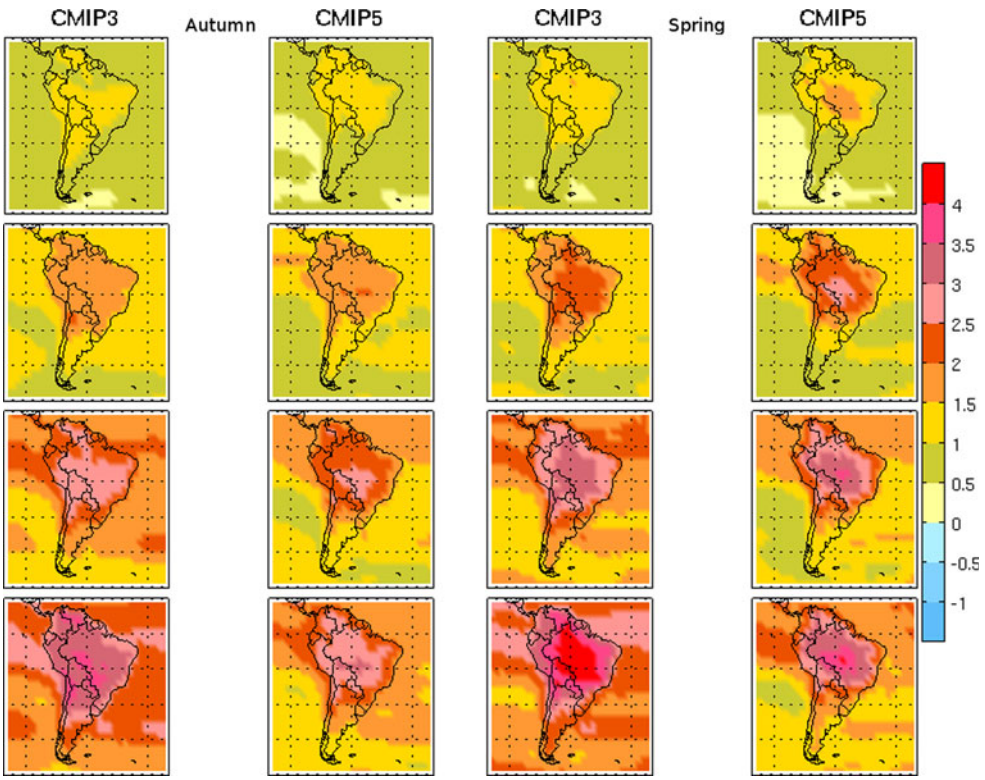

Fig. 3 Decadal mean temperature changes (relative to the average 1971–2000) (°C) for autumn and spring for the CMIP3 and CMIP5 models. 95 % confidence level (*shaded*). The *rows* (from *top* to *bottom*) indicate decades 3, 5, 7 and 9

CMIP5 (CMIP3) models perform better or have less uncertainty than CMIP3 (CMIP5) models. Figure 8 shows the ratio for internal variability for all the seasons. In general internal variability is less over the oceans in CMIP5 models (especially at high and tropical latitudes). On the continent, CMIP5 models performed best over

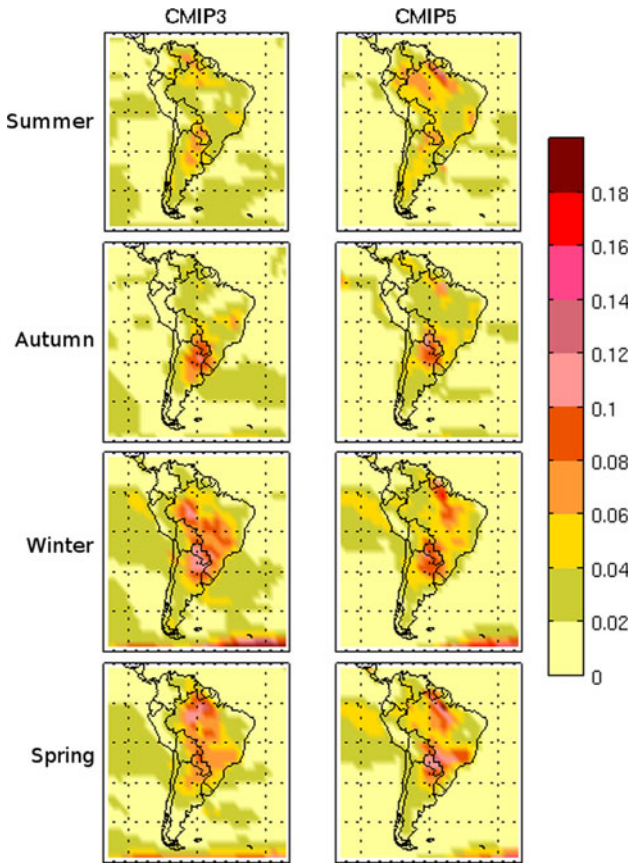

Fig. 4 Internal variability of decadal mean temperature (°C) for the CMIP3 and CMIP5 models (21st century)

eastern-central Argentina especially in summer and autumn, over high latitudes and the subtropics in winter and over the northwest of Brazil in spring.

Figure 9 shows the ratio (Eq. 6) for inter-model variability for all the seasons and for decades 3rd, 5th, 7th and 9th of 21st century. In general, inter-model variability is smaller in CMIP5 models than in CMIP3 in all seasons, which is particularly noticeable in the last decades of the current century. It is worth mentioning that this improvement is generally observed in areas where inter-model variability is not high. In the last decades, lower inter-model variability in CMIP3 models occurs in the northwest of South America in fall, winter and spring.

4.2 Precipitation

Decadal changes in precipitation (relative to the period 1971–2000) projected by CMIP3 and CMIP5 models were analysed before studying the uncertainties. Figure 10 exhibits such changes for summer and winter and Fig. 11 for autumn and spring, in the decades analysed. Changes are statistically significant in few areas (95 % confidence level). In general, models project negative changes over the central Pacific, southern-central Chile and positive changes over SESA and the southern oceans, particularly in the last decades of the century in all the seasons. However, there are some differences between the two sets of data. For example, although both models exhibit a negative change on the Pacific Ocean and central and southern Chile in autumn, only CMIP5 models show statistically significant positive changes over SESA. The opposite happens over the Amazon region in winter where only CMIP3 models show statistically significant the negative change in the last decades. Contrary to temperature, no marked differences exist in the intensity of precipitation changes in both sets of data, even when the emission scenarios used are different.

Figure 12 shows the internal variability—which had been assumed to be constant in time—for all the seasons, for both model packages. Variability peaks in CMIP3 and CMIP5 models are located over the same regions: tropical latitudes (associated to the seasonal shift of the ITCZ), southern-central Chile and SACZ (South Atlantic Convergence Zone). In general, internal variability is similar in both model packages, although CMIP5 models exhibit higher values (maximum over southern and central Chile in all the seasons and maximum over SESA in spring). The greatest internal variability is found in tropical zones (above 0.27 mm/day).

Figure 13 shows inter-model variability for summer and winter. Inter-model variability increases with time in all seasons (peaks above 1.8 mm/day in some regions and seasons). In particular, inter-model variability is smaller in CMIP5 models, in summer over the north and east of Brazil (area of maximum precipitation associated with the South American monsoon), especially in the last decades of the century. In addition, a decrease in variability is observed over the western tropical Atlantic. In autumn (not shown) variability in CMIP5 models is higher over the eastern tropical Pacific. Both packages behave similarly for winter projections, with maximum variability over the tropics. However, in the last decades of the century, CMIP5 model variability is greater over SESA (the area where winter climatological precipitation peaks). In spring (not shown), inter-model variability is higher over SESA in CMIP5 models (this region coincides with one of the secondary maxima of observed precipitation).

The relative weight (RW) of internal variability was compared in both sets of models. Figure 14 shows the RW, calculated according to Eq. 4, for summer and winter, for decades 3rd, 5th, 7th and 9th of 21st century. In both datasets internal variability decreases with time in all seasons, which is mainly noticeable in tropical and subtropical regions.

The reliability of the projections was also explored in both model sets. Figure 15 shows the signal to noise ratio (SN) for summer and winter, and for the 3rd, 5th, 7th and

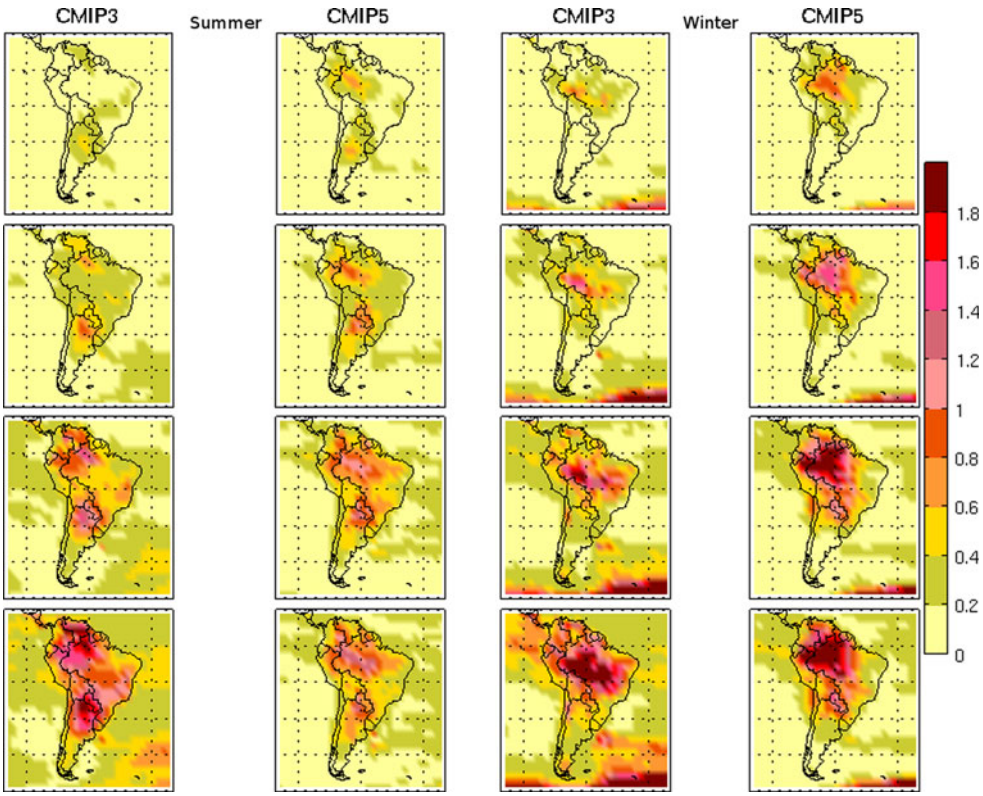

Fig. 5 Inter-model variability of decadal mean temperature (°C) for the CMIP3 and CMIP5 models (21st century). The *rows* (from *top* to *bottom*) indicate decades 3, 5, 7 and 9

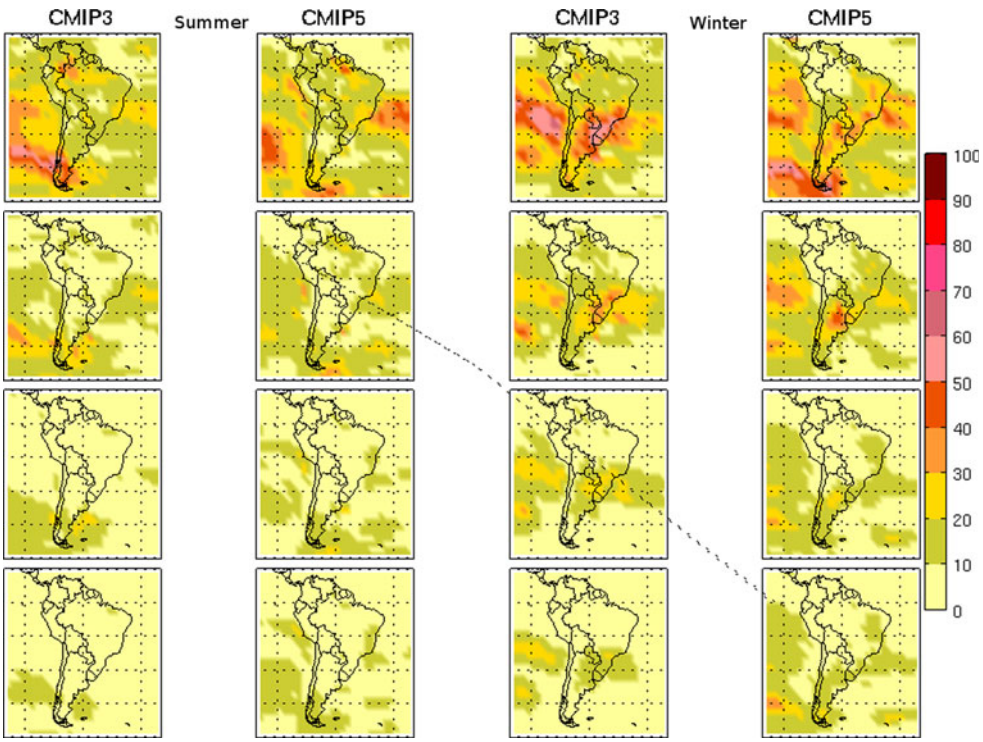

Fig. 6 Relative weights (RWs) of internal variability for decadal mean temperature (°C) for the CMIP3 and CMIP5 models (21st century). The *rows* (from *top* to *bottom*) indicate decades 3, 5, 7 and 9

9th decades of the current century. In both sets of models values are greater than 1 in all the seasons over the Atlantic and Pacific Oceans, especially at high latitudes and in the last decades of the century. This is because most models project positive changes over those regions (Fig. 10). SN summer and autumn (not shown) values are close to 1 over eastern Argentina, Uruguay and southern Brazil in all the decades included in CMIP5 models. In autumn (not shown), values are above 1 in those regions. CMIP3 models show positive values over southern Argentina and

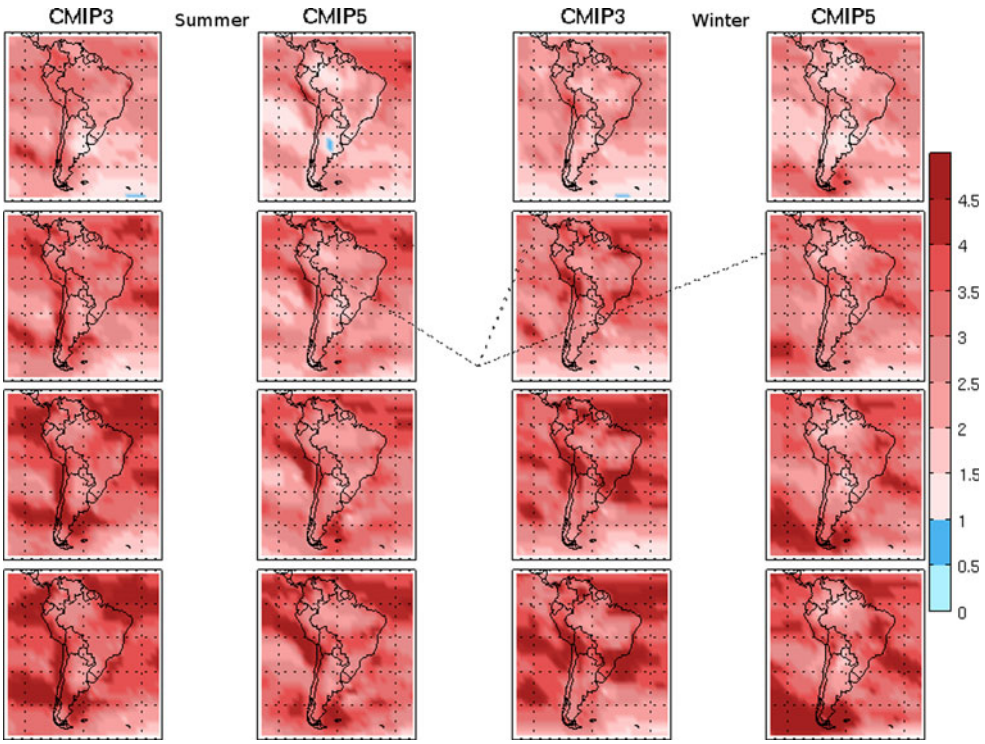

Fig. 7 Signal to noise ratio (SN) for decadal mean temperature (°C) for the CMIP3 and CMIP5 models. 95 % confidence level (*shaded*). The *rows* (from *top* to *bottom*) indicate decades 3, 5, 7 and 9

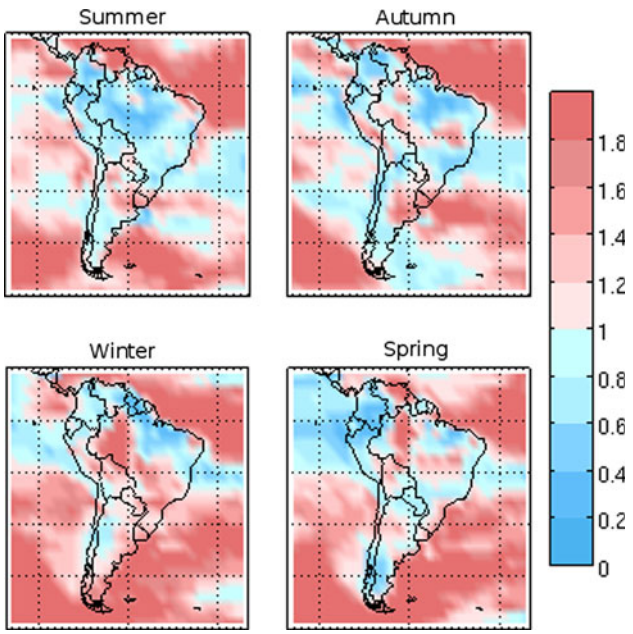

Fig. 8 Ratio for internal variability (CMIP3 variability/CMIP5 variability) for decadal mean temperature (°C) (21st century)

Chile for winter of most of the decades of the current century. In spring (not shown), both model packages behave similarly, with SN above 1 at high latitudes, and close to 1 over SESA.

Differences in uncertainties of CMIP3 and CMIP5 models were explored (Eq. 6). It is worth remembering that values above (below) 1 indicate that variability in CMIP3 models is greater (smaller) than in CMIP5. Figure 16 shows the internal variability ratio for all the seasons. During summer, the maximum internal variability over the continent is located in central and eastern Brazil (see Fig. 12), with no differences between both model packages. Over the tropical Atlantic (southern Ecuador) and northwest of the continent, CMIP5 models perform better than CMIP3. This means that in these regions, internal variability in the new generation models (CMIP5) is smaller. However, the older models perform better over northern Argentina and the western tropical Pacific. In autumn, the maximum variability is located over the tropics (see Fig. 12). There are few areas over the continent where one model set performs better than the other. For example, over northeastern Brazil and northwest of South America values are greater than 1, indicating internal variability is smaller in CMIP5 models. Over the oceans, CMIP3 models variability is smaller over the tropical Pacific. In winter, the maximum internal variability occurs over the tropical oceans and southern and central Chile (see Fig. 12). In this season, Fig. 16 shows that the variability peak is located farther to the north in the tropics in CMIP5 models. Internal variability in CMIP3 models is smaller over southern-central Chile. In spring, the maximum is located over tropical latitudes and SESA (see Fig. 12). While CMIP5 models perform better over the tropical Atlantic Ocean, the opposite occurs over SESA and the tropical Pacific (greater internal variability in new generation models).

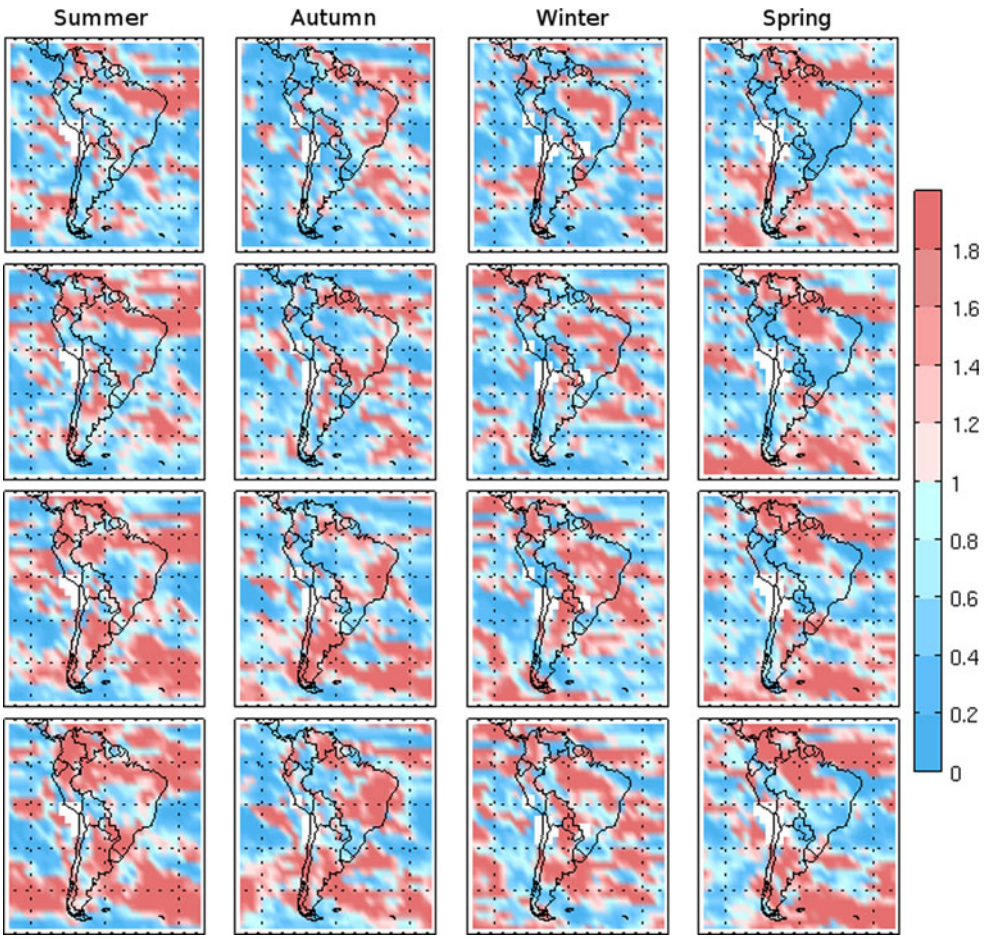

Fig. 9 Ratio for inter-model variability (CMIP3 variability/ CMIP5 variability) for decadal mean temperature (°C) (21st century). The *rows* (from *top* to *bottom*) indicate decades 3, 5, 7 and 9

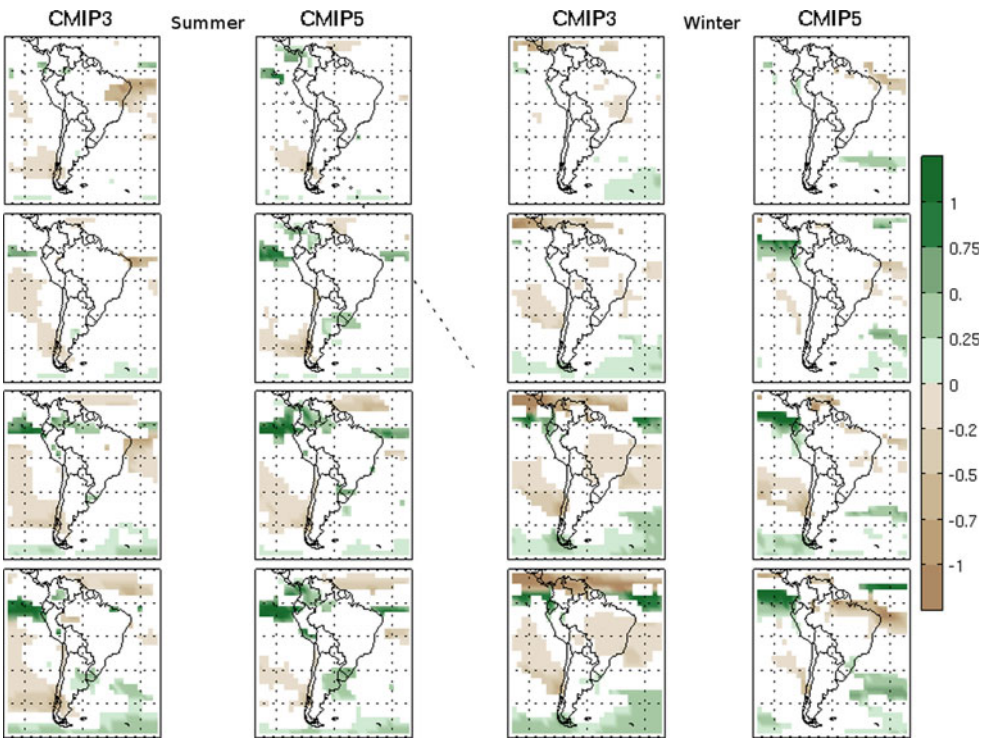

Fig. 10 Decadal mean precipitation changes (relative to the average 1971–2000) (mm/day) for summer and winter for the CMIP3 and CMIP5 models. 95 % confidence level (*shaded*). The *rows* (from *top* to *bottom*) indicate decades 3, 5, 7 and 9

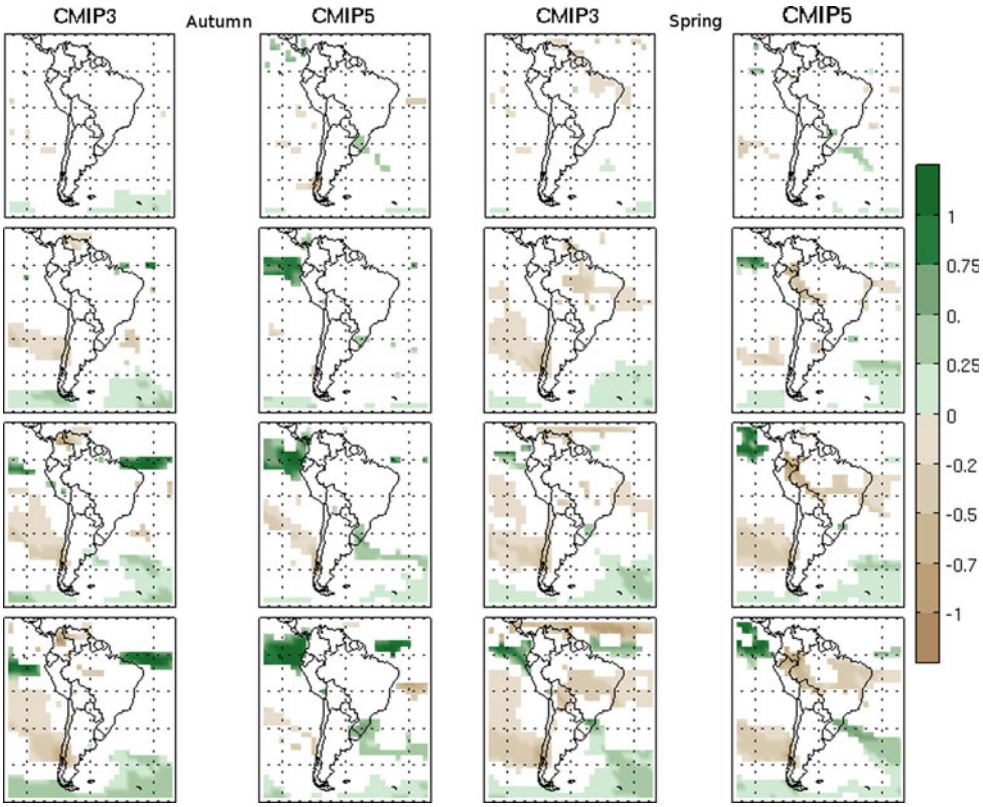

Fig. 11 Decadal mean precipitation changes (relative to the average 1971–2000) (mm/day) for autumn and spring for the CMIP3 and CMIP5 models. 95 % confidence level (*shaded*). The *rows* (from *top* to *bottom*) indicate decades 3, 5, 7 and 9

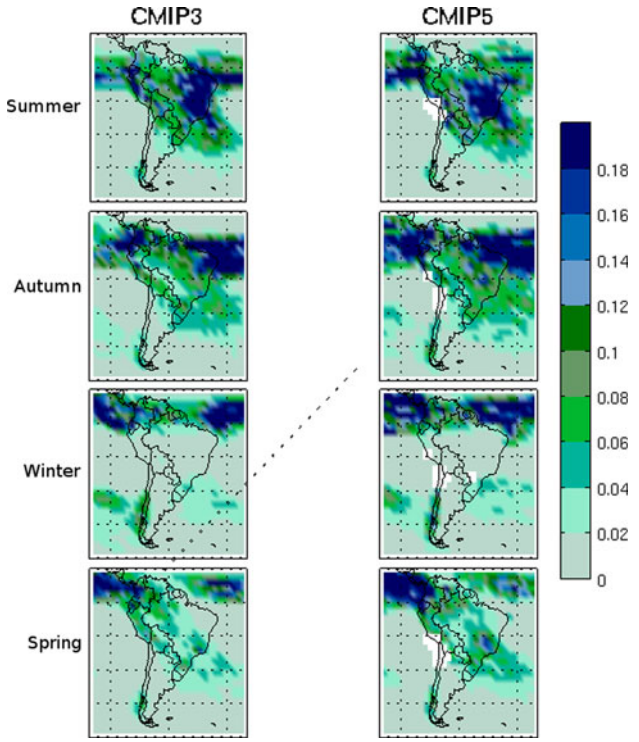

Fig. 12 Internal variability of decadal mean precipitation (mm/day) for the CMIP3 and CMIP5 models (21st century)

Figure 17 shows the ratio (Eq. 6) for inter-model variability for all the seasons and decades 3rd, 5th, 7th and 9th of the 21st century. In summer, CMIP5 models have a well perform at tropical latitudes (regions of maximum inter-model variability, Fig. 13), although the opposite occurs in central Brazil. This feature becomes more pronounced with time. In autumn, the biggest improvements in new generation model simulations are observed over northern and eastern Brazil and central and southern Argentina; although inter-model variability is smaller in the latter. This is particularly evident in the last decades of century. In winter, some improvements in the new generation of models are observed over the northern of the continent at the end of the century. Over SESA, variability in CMIP3 is less than in CMIP5 models. Finally, in spring, new generation models perform better on the northwest of the continent (area of maximum variability, Fig. 13), and the opposite is observed over SESA in most of the decades analysed.

5 Conclusions

Sources of uncertainty in climate projections from WCRP-CMIP3 and WCRP-CMIP5 models were examined. Both sets were compared to identify improvements in the new

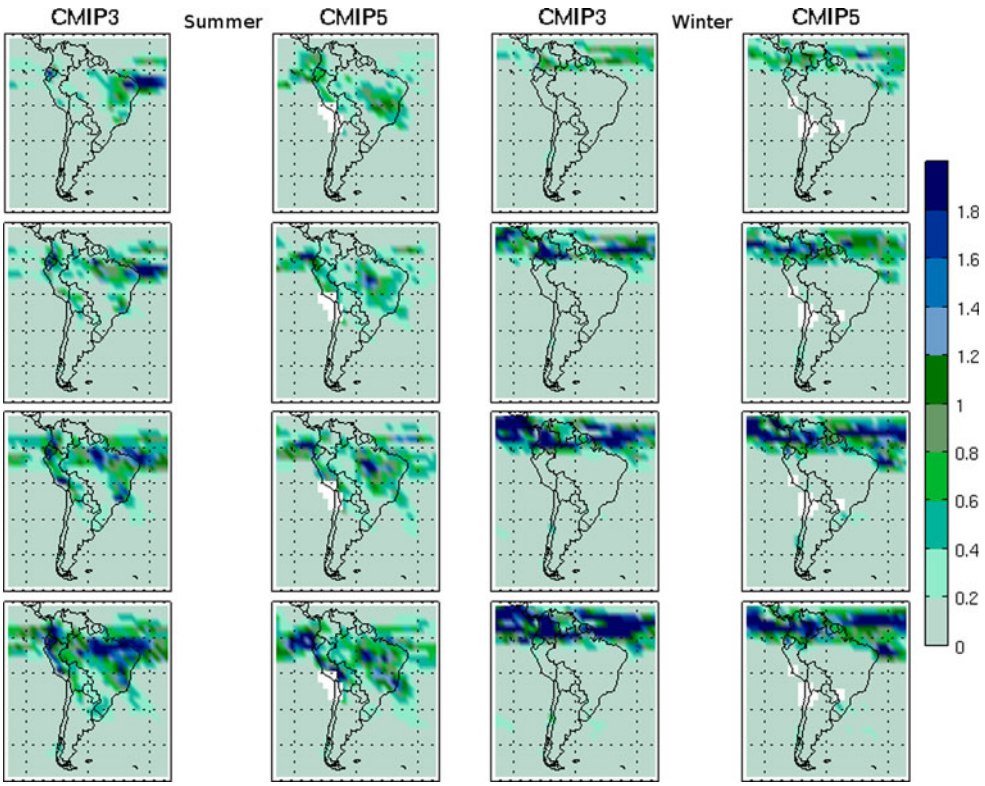

Fig. 13 Inter-model variability of decadal mean precipitation (mm/day) for the CMIP3 and CMIP5 models (21st century). The *rows* (from *top* to *bottom*) indicate decades 3, 5, 7 and 9

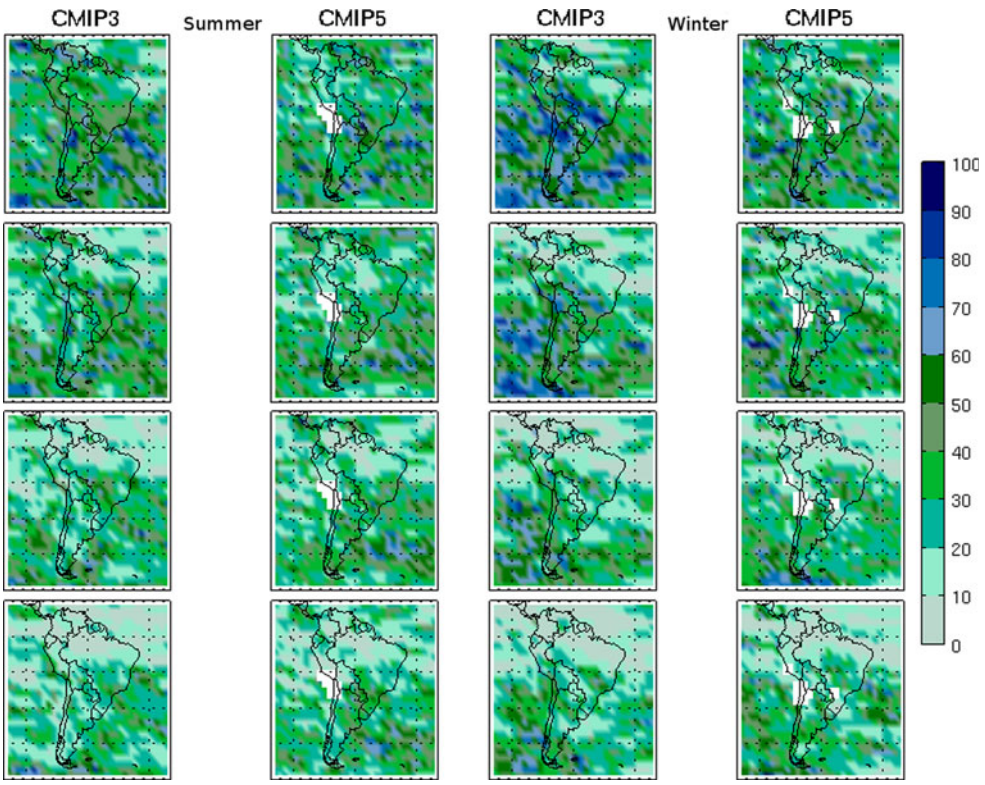

Fig. 14 Relative weights (RWs) of internal variability for decadal mean precipitation (mm/day) for the CMIP3 and CMIP5 models (21st century). The *rows* (from *top* to *bottom*) indicate decades 3, 5, 7 and 9

generation models. In particular, the sources of uncertainties due to internal and inter-model variability were analysed for both precipitation and temperature.

Both sets of models located the maximum internal variability in the same regions (over northeastern Brazil and over northeastern Argentina and Paraguay), although

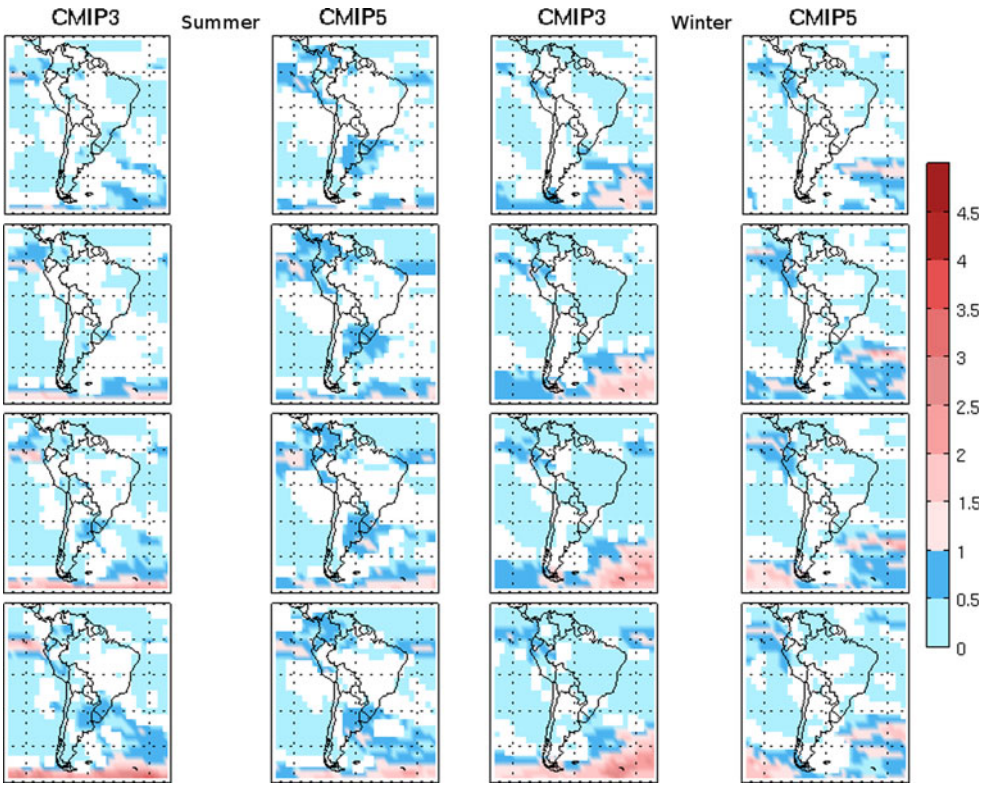

Fig. 15 Signal to noise ratio (SN) for decadal mean precipitation (mm/day) for the CMIP3 and CMIP5 models. 95 % confidence level (*shaded*). The *rows* (from *top* to *bottom*) indicate decades 3, 5, 7 and 9

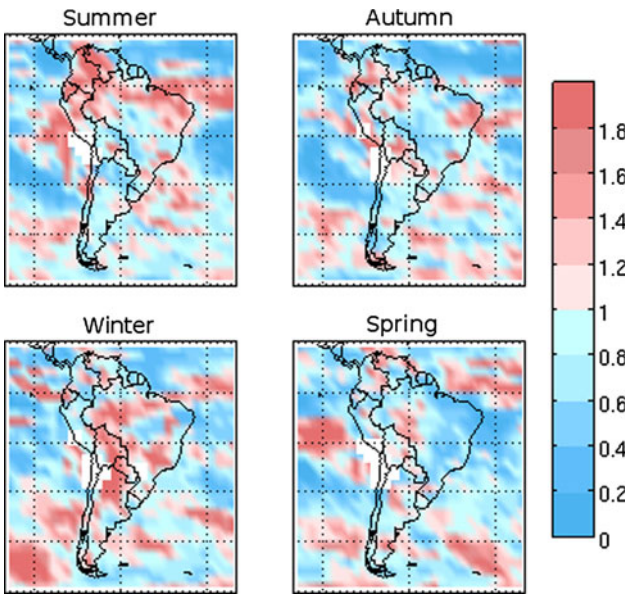

Fig. 16 Ratio for internal variability (CMIP3 variability/CMIP5 variability) for decadal mean precipitation (mm/day) (21st century)

the tropical peak in the new generation models is shifted to the east. In general, no significant changes were observed in both datasets. Inter-model temperature variability in both datasets increases with time. Even though both datasets place the maxima in the same regions (tropics and subtropics), which also coincide with the maximum projected changes, some differences were observed. For example, in summer, inter-model variability in CMIP5 models is smaller over northeastern Argentina, Paraguay and northern Brazil (areas of maximum variability) in the last decades of the century. In the other seasons, performance of CMIP5 models is worse than that of CMIP3, with greater variability in most of the decades analysed. In all seasons and in both datasets, internal variability was more important in the early decades, whereas inter-model variability became important in the last decades of the 21st century.

The signal to noise ratio was analysed in both sets of data to detect improvements in the reliability of temperature projections in the new generation models. Values were above 1 in most of the domain under study for both sets of models, which indicates temperature projections are highly reliable (this is because all models project positive changes over most of the study region). CMIP3 models have higher SN values in some areas, probably because the changes projected by CMIP3 models are greater than those projected by CMIP5 which is consistent with the higher greenhouse gas emission scenario (A1B).

The ratio of (internal or inter-model) variability was used to compare CMIP3 and CMIP5 datasets. Performance of temperature internal variability was the best in new generation models over the southern and tropical oceans in all the seasons; on eastern-central Argentina in summer and autumn; at high and subtropical latitudes of the continent in winter; in the northwest of Brazil in spring. Regarding

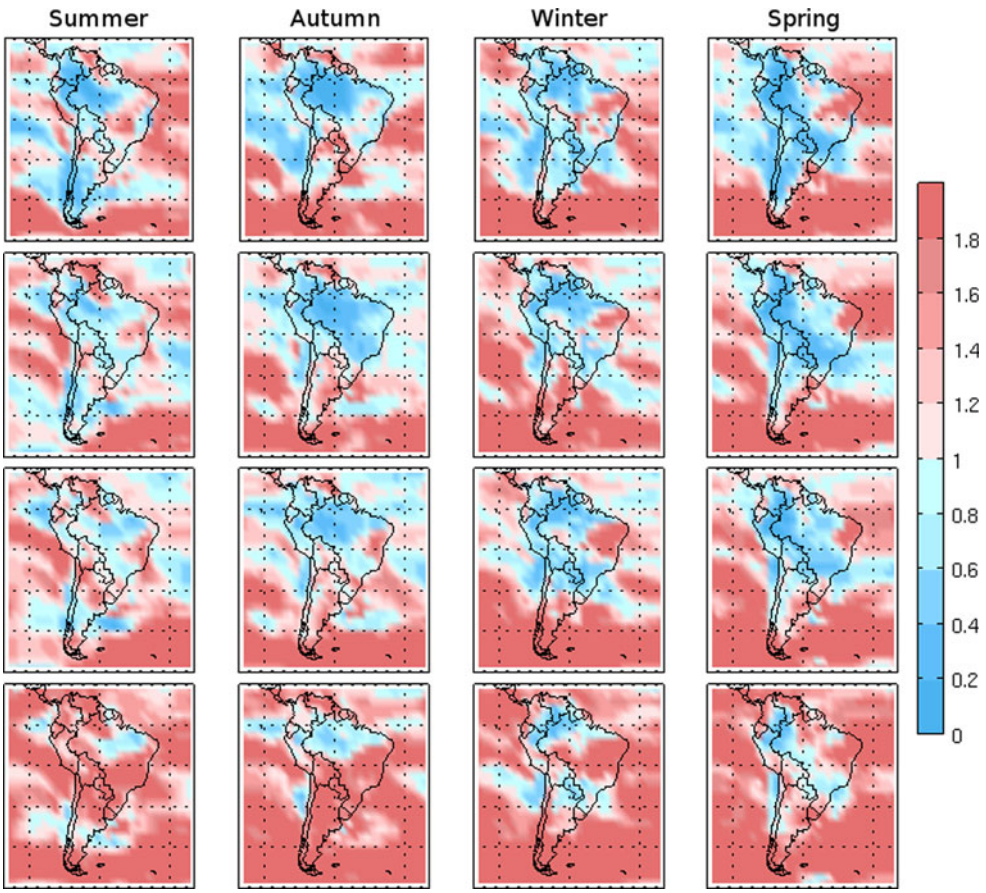

Fig. 17 Ratio for inter-model variability (CMIP3 variability/CMIP5 variability) for decadal mean precipitation (mm/day) (21st century). The *rows* (from *top* to *bottom*) indicate decades 3, 5, 7 and 9

inter-model temperature variability, improvements in the new generation models were observed especially in the last decades of the century, but areas were detected where inter-model variability was not so high.

Projected precipitation changes in both datasets were similar, despite the different emission scenarios. Both model packages showed the highest internal variability over the same regions (tropical latitudes, southern and central Chile and the SACZ area). No significant improvements were observed in CMIP5 models relative to CMIP3, but, internal variability was greater in some cases: e.g., in southern and central Chile in all seasons and SESA in spring. Both datasets show an increase in inter-model variability with time. It was found an improvement in the new generation of models during the summer with decreased variability in northern and eastern Brazil, especially in the last decades of the 21st century, which is important because this area coincides with the maximum observed precipitation. In the remaining seasons, no significant differences were observed between both model packages. Internal variability decreased with time regarding total variability in both sets of data. The signal to noise ratio for precipitation was smaller than 1 in most of the study domain in both sets of models. However, some improvements were detected in CMIP5 models. For example, in summer and autumn, SN values were close to 1 over eastern Argentina, Uruguay and southern Brazil in the new generation models, and some positive values were observed in autumn.

Both model packages were compared using the ratio of precipitation (internal or inter-model) variability. Some improvements were found in internal variability in the new generation models: in summer over the tropical Atlantic and northwest of the continent; in autumn in northeastern Brazil and northwest of the continent; in spring over the tropical Atlantic. Improvements were also observed in inter-model variability in the new generation models over tropical regions in summer, in the north and east of Brazil in autumn, in the north of the continent in winter and in northwestern South America in spring.

According to this methodology, no significant improvements in uncertainty of projections of CMIP5 were observed. Both the internal and inter-model precipitation and temperature variability decreased in some regions, but increased in others. However, this result may depend on the models selected for this analysis (a greater number of models could show major improvements) or the methodology used in this study.

The no significant improvements mainly in the inter-model variability of CMIP5 models regards to CMIP3

could be attribute to the fact that new generation models include new feedbacks (like carbon cycle) or new parameterizations (especially those refers to cumulus and radiation schemes were improved or changed in some CMIP5 models). May be these changes would lead to new sources of uncertainties. Nevertheless, different conclusions could be reached using other methodology to quantify uncertainties.

It is interesting to note that internal variability is the lower limit of uncertainty, and difficult to reduce. However, the source of uncertainty that might be reduced in the future is inter-model variability, as long as a better representation is achieved of all the physical and chemical processes in the climate system. If inter-model variability could be reduced, only internal variability and the variability between emission scenarios—which does not play a major role in precipitation projections—would have significant effects (HS11).

Acknowledgments The authors thank the World Climate Research Programme's Working Group on Coupled Modelling, in charge of CMIP, and the climate modelling groups (listed in Tables 1, 2 of this paper) for producing and making available their model outputs. For CMIP the U.S. Department of Energy's Program for Climate Model Diagnosis and Intercomparison provides coordinating support and led development of software infrastructure in partnership with the Global Organization for Earth System Science Portals. The authors are also grateful to Dr. Edward Hawkins for his help with the methodology used in this paper and two anonymous reviewers for their valuable comments that helped to improve this paper. This study was supported with grants from UBACYT-X160, PIP CONICET 112-200801-00195 and CLARIS-LPB (A Europe-South America Network for Climate Change Assessment and Impact Studies in La Plata Basin).

Appendix

The new generation models (WCRP-CMIP5) present some differences regarding the previous generation (WCRP-CMIP3). Some of them are listed below:

- CanESM2 model (Chylek et al. 2011): presents a new algorithm of radiation (k-correlated distribution, Li and Barker 2005): an improvement in the aerosol optical property parameterization, direct and indirect radiative effects in aerosols using a prognostic bulk aerosol scheme, a new shallow convection scheme (von Salzen and McFarlane 2002).
- CSIRO-Mk3.6 model (Rotstayn et al. 2010): this version includes an interactive aerosol scheme (sulfate, dust, sea salt and carbonaceous aerosol); an updated in the radiation scheme; a modification in the boundarulayer treatment (non-local scheme); some minor changes are introduced in convection and clouds schemes (including direct and indirect effects of aerosols and aerosols from volcanic eruptions).
- INM-CM4 model (Volodin et al. 2010): the time step has reduced from 12 to 5 min; the horizontal resolution is increased; some physical parameterizations have slightly changed: radiation, shallow and deep convections, orographic and nonorographic gravity waves resistances and processes related to vegetation and soil.
- IPSL-CM5A-LR (http://icmc.ipsl.fr/images/internal/ipsl-esm-20100228-1.pdf): improved horizontal resolution, inclusion of the carbon cycle; connection between tropospheric chemistry and layer.
- MIROC5 model (Watanabe et al. 2010): the vertical coordinate σ was changed to the hybrid σ-p (Arakawa and Konor 1996); the radiative scheme was updated (improvements in the line absorption and continuum absorption with an increase in the number of absorption bands from 18 to 29); the cumulus parameterization was changed (Chikira and Sugiyama 2009): it is an entraining-plume model, where the lateral entrainment rate varies vertically depending on the surrounding environment; in order to better represent cloud and cloud-radiative feedback, it was developed a prognostic LSC scheme (Watanabe et al. 2009) and a bulk microphysical scheme was implemented (Wilson and Ballard 1999); a aerosol module (SPRINTARS, Takemura et al. 2005, 2009) was coupled with the radiation and cloud microphysics schemes to calculate the direct and indirect effects of the aerosols.
- MIROC5-ESM model (Watanabe et al. 2011): based on the global climate model MIROC includes an atmospheric chemistry component (CHASER), a nutrient-phytoplankton-zooplankton-detritus (NPZD) type 10 ocean ecosystem component, and a terrestrial ecosystem component dealing with dynamic vegetation (SEIB-DGVM). This model has the fully resolved stratosphere and mesosphere (Watanabe et al. 2008). The hybrid terrain-following (sigma) pressure vertical coordinate system is used, and there are 80 vertical layers between the surface and about 0.003 hPa. In order to obtain the spontaneously generated equatorial quasi-biennial oscillation (QBO), a fine vertical resolution of about 680 m is used in the lower stratosphere. Some parameterizations were modified, especially those who are crucial for the representation of the large-scale dynamical and thermal structures in the stratosphere and mesosphere.
- MRI-CGCM3 model (Yukimoto et al. 2011): some settings were changed. For example, in the cumulus scheme (Arakawa and Schubert 1974) a prognostic mass flux method is used to express the condition of away from quasi-equilibrium (Randall and Pan 1993; Pan and Randall 1993, 1998). The cumulus downdraft is also considered (Cheng and Arakawa 1997). A mid-level

convection scheme is included to express the mid-latitude convection accompanying the front and synoptic-scale disturbances. In the radiative scheme, the short and long wave radiation are treated separately. The long-wave (short-wave) region of the spectrum is divided into 9 (22) bands. The radiative flux is calculated in each band. In the cloud scheme, the model can recognize the spatial and temporal distribution of aerosols due to coupling between the aerosol model and the chemistry. It was implemented a new soil model (HAL; Hosaka 2011).

- HadGEM2-ES model (Martin et al. 2011, Collins et al. 2009): it was implemented an adaptive detrainment parameterization in the convection scheme, which improves the simulation of tropical convection and leads to a much reduced (and more realistic) wind stress over the tropical Pacific, and a package of changes including an alteration to the treatment of excess water from super-saturated soil surfaces and improved representation of the lifetime of convective cloud. Several changes and additions to the representation of aerosol have been carried out. Improvements include changes to existing aerosol species, such as sulphate and biomass-burning aerosols, and representation of additional species, such as mineral dust, fossil-fuel organic carbon, and secondary organic aerosol from biogenic terpene emissions. New Earth System components include the terrestrial and oceanic ecosystems and tropospheric chemistry. The ecosystem components are introduced principally to allow simulation of the carbon cycle and its interactions with climate.

References

Arakawa A, Konor CS (1996) Vertical differencing of the primitive equations based on the Charney-Phillips grid in hybrid σ-p vertical coordinates. Mon Weather Rev 124:511–528

Arakawa A, Schubert WH (1974) Interaction of a cumulus cloud ensemble with the large-scale environment; Part I. J Atmospheric Sci 31:674–701. doi:10.1175/1520-0469(1974)031<0674:IOACCE>2.0.CO;2

Bidegain M, Camilloni I (2006) Performance of GCMs and climate future scenarios for southeastern South America. In: Proceedings of the 8th international conference on southern hemisphere meteorology and oceanography, 24–28 April, 2006, Foz do Iguaçu, Brazil

Blázquez J, Nuñez MN, Kusunoki S (2012) Climate projections and uncertainties over South America from MRI/JMA global model experiments. Atmos Clim Sci (in press)

Cabré MF, Solman S, Nuñez MN (2010) Creating regional climate change scenarios over southern South America for the 2020's and 2050's using the pattern caling technique: validity and limitations. Clim Change 98:449–469. doi:10.1007/s10584-009-9737-5

Carril AF, Menéndez CG, Nuñez MN (1997) Climate change scenarios over the South American region: an intercomparison of coupled general atmosphere-ocean circulation models. Int J Climatol 17:1613–1633. doi:10.1002/(SICI)1097-0088(199712)17:15<1613:AID-JOC209>3.0.CO;2-8

Cheng MD, Arakawa A (1997) Inclusion of rainwater budget and convective downdrafts in the Arakawa–Schubert cumulus parameterization. J Atmos Sci 54:1359–1378. doi:10.1175/1520-0469(1997)054<1359:IORBAC>2.0.CO;2

Chikira M, Sugiyama M (2009) A cumulus parameterization with state-dependent entrainment rate. Part I: description and sensitivity to temperature and humidity profiles. J Atmos Sci 67:2171–2193. doi:10.1175/2010JAS3316.1

Chylek P, Li J, Dubey MK, Wang M, Lesins G (2011) Observed and model simulated 20th century Arctic temperature variability: Canadian Earth System Model CanESM2. Atmos Chem Phys 11:22893–22907. doi:10.5194/acpd-11-22893-2011

Collins WJ, Bellouin N, Doutriaux-Boucher M, Gedney N, Hinton T, Jones CD, Liddicoat S, Martin G, O'Connor F, Rae J, Senior C, Totterdell I, Woodward S, Reichler T, Kim J (2009) Evaluation of HadGEM2 Model. Met Office, Exeter. Hadley Centre Technical Note 74

Cox P, Stephenson D (2007) A changing climate for prediction. Science 317:207–208. doi:10.1126/science.1145956

Flato GM (2005) The Third Generation Coupled Global Climate Model (CGCM3). Available online en http://www.cccma.bc.ec.gc.ca/models/cgcm3.shtml

Garreaud R, Falvey M (2008) The coastal winds off western subtropical South America in future climate scenarios. Int J Climatol 29:543–554. doi:10.1002/joc.1716

Giorgi F, Bi X (2009) Time of emergence (TOE) of GHG-forced precipitation change hot-spots. Geophys Res Lett 36:L06709. doi:10.1029/2009GL037593

Giorgi F, Francisco R (2000) Uncertainties in Regional Climate Change Prediction: a regional analysis of ensemble simulations with the HADCM2 coupled AOGCM. Clim Dyn 16:169–182. doi:10.1007/PL00013733

Giorgi F, Mearns LO (2002) Calculation of average uncertainty range, and reliability of regional climate changes from AOGCM simulations via the "reliability ensemble averaging" (REA) method. J Clim 15:1141–1158. doi:10.1175/1520-0442(2002)015<1141:COAURA>2.0.CO;2

Gordon HB, Rotstayn LD, McGregor JL, Dix MR, Kowalczyk EA, O'Farrell SP, Waterman LJ, Hirst AC, Wilson SG, Collier MA, Watterson IG, Elliott TI (2002) The CSIRO Mk3 climate system model. Aspendale: CSIRO atmospheric research, CSIRO Atmospheric Research technical paper; no. 60, 130 pp. (http://www.dar.csiro.au/publications/gordon_2002a.pdf)

Hasumi H, Emori S (eds) (2004) K-1 coupled model (MIROC) description, K-1 technical report, 1, Center for climate system research, University of Tokyo, 34 pp. Available at http://www.ccsr.u-tokyo.ac.jp/kyosei/hasumi/MIROC/tech-repo.pdf

Hawkins E, Sutton R (2009) The potential to narrow uncertainty in regional climate predictions. Bull Am Meteorol Soc 90:1095–1107. doi:10.1175/2009BAMS2ensamblede607.1

Hawkins E, Sutton RT (2011) The potential to narrow uncertainty in projections of regional precipitation change. Clim Dyn 37:407–418. doi:10.1007/s00382-010-0810-6

Hosaka (2011) MRI New land surface model HAL. The Second Symposium on Polar Science "The Front Line of Ice Core Studies" Program. Disponible en: http://www.nipr.ac.jp/symposium2011/program/Pmg/P_HosakaMasahiro_P.pdf

Johns TC, Durman CF, Banks HT, Roberts MJ, McLaren AJ, Ridley JK, Senior CA, Williams KD, Jones A, Rickard GJ, Cusack S, Ingram WJ, Crucifix M, Sexton DMH, Joshi MM, Dong BW,

Spencer H, Hill RSR, Gregory JM, Keen AB, Pardaens AK, Lowe JA, Bodas-Salcedo A, Stark S, Searl Y (2006) The new Hadley Centre climate model HadGEM1: evaluation of coupled simulations. J Clim 19:1327–1353

Kitoh A, Kusunoki S, Nakaegawa T (2011) Climate change projections over South America in the late 21st century with the 20 and 60 km mesh Meteorological Research Institute atmospheric general circulation model (MRI-AGCM). J Geophys Res 116:D06105. doi:10.1029/2010JD014920

Knutti R, Allen MR, Friedlingstein P, Gregory JM, Hegerl GC, Meehl GA, Meinshausen M, Murphy JM, Plattner GK, Raper SCB, Stocker TF, Stott PA, Teng H, Wigley TLM (2008) A review of uncertainties in global temperature projections over the twenty-first century. J Clim 21:2651–2663. doi:10.1175/2007JCLI2119.1

Labraga LC, Lopez M (1997) A comparison of the climate response to increased carbon dioxide simulated by general circulation models with mixed-layer and dynamic ocean representations in the region of South America. Int J Climatol 17:1635–1650. doi:10.1002/(SICI)1097-0088(199712)17:15<1635:AID-JOC223>3.0.CO;2-G

Li J, Barker HW (2005) A radiation algorithm with correlated k-distribution. Part I: local thermal equilibrium. J Atmos Sci 62:286–309. doi:10.1175/JAS-3396.1

Marengo JA, Ambrizzi T, Rocha RP, Alves LM, Cuadra SV, Valverde MC, Ferraz SET, Torres RR, Santos DC (2009a) Future change of climate in South America in the late XXI century: intercomparison of scenarios from three regional climate models. Clim Dyn 33:1073–1097. doi:10.1007/s00382-009-0721-6

Marengo JA, Jones R, Alves LM, Valverde MC (2009b) Future change of temperature and precipitation extremes in South America as derived from the PRECIS regional climate modeling system. Int J Climatol 29:2241–2255. doi:10.1002/joc.1863

Marengo JA, Chou SC, Kay G, Alves LM, Pesquero JF, Soares WR, Santos DC, Lyra AA, Sueiro G, Betts R, Chagas DJ, Gomes JL, Bustamante JF, Tavares P (2011) Development of regional future climate change scenarios in South America using the Eta CPTEC/HadCM3 climate change projections: climatology and regional analyses for the Amazon, Sao Francisco and the Parana River basins. Clim Dyn. doi:10.1007/s00382-011-1155-5

Marti O, Braconnot P, Bellier J, Benshila R, Bony S, Brockmann P, Cadule P, Caubel A, Denvil S, Dufresne JL, Fairhead L, Filiberti MA, Foujols MA, Fichefet T, Friedlingstein P, Gosse H, Grandpeix JY, Hourdin F, Krinner G, Lévy C, Madec G, Musat I, de Noblet N, Polcher J, Talandier C (2005) The new IPSL climate system model: IPSLCM4. Tech. rep., Institut Pierre Simon Laplace des Sciences de l'Environnement Global, IPSL, Case 101, 4 place Jussieu, Paris, France

Martin GM, Bellouin N, Collins WJ, Culverwell ID, Halloran PR, Hardiman SC, Hinton TJ, Jones CD, McDonald RE, McLaren AJ, O'Connor FM, Roberts MJ, Rodriguez JM, Woodward S, Best MJ, Brooks ME, Brown AR, Butchart N, Dearden C, Derbyshire SH, Dharssi I, Doutriaux-Boucher M, Edwards JM, Falloon PD, Gedney N, Gray LJ, Hewitt HT, Hobson M, Huddleston MR, Hughes J, Ineson S, Ingram WJ, James PM, Johns TC, Johnson CE, Jones A, Jones CP, Joshi MM, Keen AB, Liddicoat S, Lock AP, Maidens AV, Manners JC, Milton SF, Rae JGL, Ridley JK, Sellar A, Senior CA, Totterdell IJ, Verhoef A, Vidale PL, Wiltshire A (2011) The HadGEM2 family of Met Office Unified Model Climate configurations. Geosci Model Dev Discuss 4:765–841. doi:10.5194/gmdd-4-765-2011

Meehl GA, Covey C, Delworth T, Latif M, McAvaney B, Mitchell JFB, Stouffer RJ, Taylor KE (2007) The WCRP CMIP3 multimodel dataset: a new era in climate change research. Bull Am Meteorol Soc 88(9):1383–1394. doi:10.1175/BAMS-88-9-1383

Moss RH, Babiker M, Brinkman S, Calvo E, Carter T, Edmonds J, Elgizouli I, Emori S, Erda L, Hibbard K, Jones R, Kainuma M, Kelleher J, Lamarque JF, Manning M, Matthews B, Meehl J, Meyer L, Mitchell J, Nakicenovic N, O'Neill B, Pichs R, Riahi K, Rose S, Runci P, Stouffer R, van Vuuren D, Weyant J, Wilbanks T, van Ypersele JP, Zurek M (2008) Towards new scenarios for analysis of emissions, climate change, impacts, and response strategies. Intergovernmental Panel on Climate Change, Geneva

Moss RH, Edmonds JA, Hibbard KA, Manning MR, Rose SK, van Vuuren DP, Carter TR, Emori S, Kainuma M, Kram T, Meehl GA, Mitchell JFB, Nakicenovic N, Riahi K, Smith SJ, Stouffer RJ, Thomson AM, Weyant JP, Wilbanks TJ (2010) The next generation of scenarios for climate change research and assessment. Nature 463:747–756. doi:10.1038/nature08823

Murphy JM, Sexton DMH, Barnett DN, Jones GS, Webb MJ, Collins M, Stainforth DA (2004) Quantification of modelling uncertainties in a large ensemble of climate change simulations. Nature 430:768–772. doi:10.1038/nature02771

Nakicenovic N, Alcamo J, Davis G, de Vries B, Fenhann J, Gaffin S, Gregory K, Grübler A, Jung TY, Kram T, Lebre La Rovere E, Michaelis L, Mori S, Morita T, Pepper W, Pitcher H, Price L, Riahi K, Roehrl A, Rogner HH, Sankovski A, Schlesinger M, Shukla P, Smith S, Swart R, van Rooijen S, Victor N, Dadi Z (2000) Special Report on Emissions Scenarios. Cambridge University Press, Cambridge

Nuñez MN, Solman SA, Cabré MF (2009) Regional climate change experiments over southern South America. II: climate change scenarios in the late twenty-first Century. Clim Dyn 32:1081–1095. doi:10.1007/s00382-008-0449-8

Pan DM, Randall DA (1993) Implementation of the Arakawa-Schubert cumulus parameterization with a prognostic closure. Meteorol Monogr 46:137–144

Pan DM, Randall DA (1998) A cumulus parameterization with a prognostic closure. Q J R Meteorol Soc 124:949–981. doi:10.1002/qj.49712454714

Randall D, Pan DM (1993) Implementation of the Arakawa-Schubert cumulus parameterization with a prognostic closure. Meteorological monograph/the representation of cumulus convection in numerical models. J Atmos Sci 46:137–144. doi:10.1007/s00382-008-0449-8

Rotstayn L, Collier M, Dix M, Feng Y, Gordon HO, Farrell S, Smith I, Syktus J (2010) Improved simulation of Australian climate and ENSO-related climate variability in a GCM with an interactive aerosol treatment. Int J Climatol 30:1067–1088. doi:10.1002/joc.1952

Soares W, Marengo J (2008) Assessments of moisture fluxes east of the Andes in South America in a global warming scenario. Int J Climatol 29:1395–1414. doi:10.1002/joc.1800

Solomon S, Qin D, Manning M, Chen Z, Marquis M, Averyt K, Tignor MMB, Miller HL (eds) (2007) Climate change 2007: the physical science basis. Cambridge University Press, Cambridge

Takemura T, Nozawa T, Emori S, Nakajima TY, Nakajima T (2005) Simulation of climate response to aerosol direct and indirect effects with aerosol transport-radiation model. J Geophys Res 110:D02202. doi:10.1029/2004JD005029

Takemura T, Egashira M, Matsuzawa K, Ichijo H, O'ishi R, Abe-Ouchi A (2009) A simulation of the global distribution and radiative forcing of soil dust aerosols at the Last Glacial Maximum. Atmos Chem Phys 9:3061–3073

Taylor KE, Stouffer RJ, Meehl GA (2012) An overview of CMIP5 and the experiment design. Bull Am Meteorol Soc 93:485–498. doi:10.1175/BAMS-D-11-00094.1

Urrutia R, Vuille M (2009) Climate change projections for the tropical Andes using a regional climate model: temperature and precipitation simulations for the end of the 21st century. J Geophys Res 114:D02108. doi:10.1029/2008JD011021

Vera C, Silvestri G, Liebmann B, Gonzalez P (2006) Climate change scenarios for seasonal precipitation in South America from IPCC-AR4 models. Geophys Res Lett 33:L13707. doi:10.1029/2006GL025759

Vera C, Gonzalez PLM, Silvestri G (2009) About uncertainties in WCRP/CMIP3 climate simulations over South America. In: Proceedings of the 9th international conference on southern hemisphere meteorology and oceanography. 9–13 February, 2009, Melbourne, Australia

Volodin EM, Diansky NA (2004) El-Niño reproduction in coupled general circulation model of atmosphere and ocean. Russ Meteorol Hydrol 12:5–14

Volodin EM, Diansky NA, Gusev AV (2010) Simulating present day climate with the INMCM4.0 Coupled Model of the atmospheric and oceanic general circulations. Izvestiya Atmos Ocean Phys 46:414–431. doi:10.1134/S000143381004002X

von Salzen K, McFarlane N (2002) Parameterization of the bulk effects of lateral and cloud-top 10 entrainment in transient shallow cumulus clouds. J Atmos Sci 59:1405–1429. doi:10.1175/1520-0469(2002)059<1405:POTBEO>2.0.CO;2

Watanabe S, Miura H, Sekiguchi M, Nagashima T, Sudo K, Emori S, Kawamiya M (2008) Development of an atmospheric general circulation model for integrated Earth system modeling on the Earth simulator. J Earth Simul 9:28–35

Watanabe M, Emori S, Satoh M, Miura H (2009) A PDF-based hybrid prognostic cloud scheme for general circulation models. Clim Dyn 33:795–816. doi:10.1007/s00382-008-0489-0

Watanabe M, Suzuki T, O'ishi R, Komuro Y, Watanabe S, Emori S, Takemura T, Chikira M, Ogura T, Sekiguchi M, Takata K, Yamazaki D, Yokohata T, Nozawa T, Hasumi H, Tatebe H, Kimoto M (2010) Improved climate simulation by MIROC5: mean states, variability, and climate sensitivity. J Clim 23:6312–6335. doi:10.1175/2010JCLI3679.1

Watanabe S, Hajima T, Sudo K, Nagashima T, Takemura T, Okajima H, Nozawa T, Kawase H, Abe M, Yokohata T, Ise T, Sato H, Kato E, Takata K, Emori S, Kawamiya M (2011) MIROC-ESM: model description and basic results of CMIP5-20c3 m experiments. Geosci Model Dev Discuss 4:1063–1128. doi:10.5194/gmdd-4-1063-2011

Wilson DR, Ballard SP (1999) A microphysically based precipitation scheme for the UK meteorological office unified model. Q J R Meteorol Soc 125:1607–1636. doi:10.1002/qj.49712555707

Yukimoto S, Noda A (2002) Improvements of the meteorological research institute global ocean-atmosphere coupled GCM (MRI-CGCM2) and its climate sensitivity. Technical report 10, NIES, Japan

Yukimoto S, Yoshimura H, Hosaka M, Sakami T, Tsujino H, Hirabara M, Tanaka TY, Deushi M, Obata A, Nakano H, Adachi Y, Shindo E, Yabu S, Ose T, Kitoh A (2011) Meteorological Research Institute-Earth System Model Version 1 (MRI-ESM1). Model description. Technical Reports of the Meteorological Research Institute, No. 64